Supplementary Information (SI) for ChemComm.

This journal is © The Royal Society of Chemistry 2026

Supporting Information (SI)

Fluorinated Zr-MOFs Supported Cu(I) for Synergistic Four-Component CO_2 Reactions

Jia Zhang, [a] Shuangfeng Yang, [a] Ruiqi Li,*[b] Yaqi Li, [a] Shiyuan Wei, [a] Jianhui Zhu, [a] Jiawei Li,*[a] Jianhan Huang*[a], and Shengze Yu [b]

a. College of Chemistry and Chemical Engineering, Central South University, Changsha, P. R. China.

b. Guangdong Advanced Carbon Materials Co., Ltd, Zhuhai, Guangdong 519000, China.

Section S1. Experimental

Materials

All chemicals were purchased from commercial suppliers and used as received. Anhydrous zirconium chloride ($ZrCl_4$), benzoic acid, anhydrous copper sulfate ($CuSO_4$), potassium iodide (KI), L-ascorbic acid (AA), organic ligand 1, 3, 6, 8-tetra(4-carboxyphenyl)pyrene (H_4TBAPy), and perfluoroalkyl carboxylic acids for surface functionalization, including trifluoroacetic acid, heptafluorobutyric acid, and undecafluorohexanoic acid. Substrates such as phenylacetylene, benzaldehyde, and n-butylamine were purchased from [Adamas]. N,N-dimethylformamide (DMF), ethanol, n-hexane, and ethyl acetate were all analytical grade and purchased from [Aladdin]. Carbon dioxide (CO_2, 99.999%) was used as supplied. Deionized water was used throughout the process. Silica gel (200–300 mesh) for column chromatography was purchased from [leyan]. Hydrochloric acid (HCl) and acetone were purchased from Kolon Chemical Co., Ltd.

Characterization

At room temperature, powder X-ray diffraction (PXRD) patterns were recorded using an Advance D8 X-ray diffractometer equipped with a Ni-filtered Cu Kα radiation source (40 kV, 100 mA) at a scanning speed of 10 °·min-1. ^{1}H NMR and ^{13}C NMR spectra were acquired using a Bruker AM 400 (400 MHz) NMR spectrometer. Infrared (IR) spectra were measured using a Thermo Scientific Nicolet iN10 MX micro-IR spectrometer at room temperature via the KBr pellet method in the range of 4000 to 400 cm^{-1}. Metal ion content was determined by inductively coupled plasma optical emission spectroscopy (ICP-OES). The pore structure of the material was characterized using N_2 adsorption-desorption isotherms at 77 K with a Micromeritics ASAP 2460 surface area analyzer. The specific surface area (SBET) of the polymer was calculated using the BET model within the range P/Po = 0.05–0.30. The total pore volume (Vtotal) was determined from the isotherm at P/Po = 0.99. The pore size distribution (PSD), microporous area (Smicro), and microporous volume (Vmicro) were all calculated using the non-local density functional theory (NLDFT) method. X-ray photoelectron spectroscopy (XPS) experiments were performed using a Thermo ESCALAB spectrometer equipped with an Al K-α radiation source. Scanning electron microscopy (SEM) testing was performed on a JSM-7610FPlus microscope at an acceleration voltage of 10 kV. Transmission electron microscopy (TEM) testing was performed on a JEOL/JEM-F200 microscope at an acceleration voltage of 80–200 kV. Substrate adsorption experiments employed a UV-2600i spectrophotometer to convert absorbance to concentration, while CO_2 adsorption-desorption isotherms were measured using a Kubo X1000 pore size and specific surface area analyzer.

Synthesis of CuI nanoparticles

Add 15 mL of ultrapure water, 5 mL of 0.15 M copper sulfate aqueous solution, 15 mL of 0.005 M ascorbic acid (AA) aqueous solution, and 5 mL of 0.15 M potassium iodide aqueous solution sequentially to the stirrer while maintaining continuous stirring. The resulting mixture was stirred for 2 hours at room temperature in a 50 mL round-bottom flask. The solid was separated by filtration and dried under vacuum to obtain the product.[1]

Preparation of NU-1000

Place 70 mg of anhydrous $ZrCl_4$ (0.30 mmol) and 2700 mg of benzoic acid (22 mmol) in 8 mL of DMF (in a 6-dram glass vial) and sonicate until clear. The clear solution was heated in an 80 °C oven for 1 hour. After cooling to room temperature, 40 mg H_4TBAPy (0.06 mmol) was added and sonicated for 20 minutes. The resulting yellow suspension was heated in a 120 °C oven for 48 hours. Upon cooling to approximately 50 °C, the supernatant was decanted, and the yellow polycrystalline material was separated by filtration. This material was activated by soaking in DMF at room temperature for 8 hours, followed by washing with fresh DMF and treatment with HCl.[2]

Activation procedure for NU-1000

Take approximately 40 mg of solvent-dispersed NU-1000 ("wet sample") and immerse it in 12 mL of DMF. Add 0.5 mL of 8 M aqueous HCl solution. Heat the mixture in a 100 °C oven for 24 hours. After cooling to approximately 50 °C, decant the supernatant. Allow the material to soak in DMF for an additional 12 h, then wash twice with DMF to remove HCl impurities. The solid residue is subsequently soaked in acetone for 12 h, washed twice with acetone, and soaked again

in acetone for 12 h. NU-1000 was filtered, briefly dried on filter paper, and activated under vacuum at 120 ºC for 12 h. The 1H NMR spectrum of the digested sample indicated that the benzoic acid ligand had been removed from the Zr_6 node and successfully introduced into the -OH group.

Preparation of CuI@NU-1000

Add 50 mg of NU-1000 to a 10 mL glass sample vial. stir overnight at room temperature with 10 mL of 0.01 M $CuSO_4$ aqueous solution. Wash the surface copper sulfate solution with fresh deionized water, centrifuge to remove the supernatant. Prepare 0.02 M KI aqueous solution and 0.02 M ascorbic acid aqueous solution. Mix equal volumes of the KI solution and ascorbic acid solution. Slowly add 10 mL of this mixed solution to the wet sample and react for 2 hours. Centrifuge to collect the solid, wash twice with deionized water, wash twice with acetone, then vacuum dry at 60 ºC for 24 hours to obtain CuI@NU-1000.

Preparation of CuI@NU-1000-F_x(x=3,7,11)

Place 60 mg of CuI@NU-1000 into a 10 mL glass vial. Add 2.4 mL of a 0.1 M perfluoroalkyl carboxylic acid (e.g., trifluoroacetic acid, heptafluorobutyric acid, undecafluorohexanoic acid) solution in acetone. Stir at room temperature for 24 h. Centrifuge to separate, wash three times with acetone, then vacuum dry at 60 ºC for 24 h to obtain CuI@NU-1000-F_x.

To ensure a stable and controllable fluorine loading level in fluorinated NU-1000 materials, a strictly standardized experimental procedure was adopted for all fluorination batches. First, NU-1000 was activated under vacuum at 120 °C for 12 h to ensure a consistent number of active sites. Subsequently, the mass of NU-1000, molar ratio of the fluorinating reagent, solvent volume, reaction temperature (60 °C), and reaction time (24 h) were kept constant. The workup procedure

employed identical washing solvents and cycles, accompanied by uniform vacuum drying conditions. The fluorine content of each batch was determined by ^{1}H and ^{19}F NMR spectroscopy of digested samples, ensuring that the relative error of fluorine loading between different batches was less than 5%, thereby guaranteeing the consistency of fluorine content and the reliability of catalytic results.

General Procedure for the Catalytic Reactions

In a sealed test tube equipped with a magnetic stir bar, 51.0 mg of CuI@NU-1000-F_x (10 mol% Cu) was placed. The reaction vessel was sealed and carbon dioxide was introduced. A carbon dioxide balloon was attached to the test tube and filled with ethanol (0.18 mL), aldehyde 2a (0.18 mL, 1.8 mmol), and amine 3a (0.18 mL, 1.8 mmol). The reaction mixture was gently stirred at room temperature for approximately 30 seconds, followed by the addition of alkyne 1a (0.100 mL, 0.892 mmol). The test tube was placed in an oil bath set at 75 °C and allowed to stand overnight. After cooling to room temperature, the reaction mixture was filtered through a silica stopper. The crude reaction mixture was further purified by silica gel column chromatography (hexane/ethyl acetate) to afford the desired oxazolidinone.[3]

Computational details

All geometry optimizations of the chiral structures (reactants, intermediates, and products) as well as the location of transition states were performed using the ORCA quantum chemistry program package. For each reaction pathway, the lowest-energy conformer was first identified and selected as the starting structure. The corresponding transition state was then located employing the Nudged Elastic Band (NEB) method, followed by full transition state optimization and verification via frequency analysis (one imaginary frequency corresponding to the reaction

coordinate). All calculations were carried out at the DFT level using the B3LYP hybrid functional. The def2-TZVP basis set was employed for all atoms, with the f functions removed (def2-TZVP(-f)) since no atoms in the present system possess occupied f orbitals. The DFT-D4 method (Grimme's D4 dispersion correction with the default Becke–Johnson damping function) was included to account for intramolecular and intermolecular dispersion interactions. Solvent effects were incorporated by means of the Conductor-like Polarizable Continuum Model (CPCM) using the corresponding experimental solvent parameters. Optimized stationary points and transition states were visualized using the VESTA software.

Section S2. General Characterization

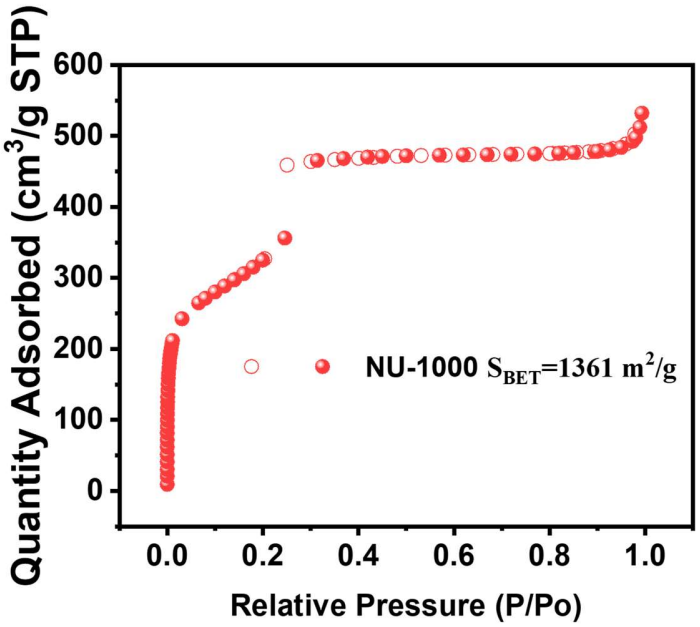

Fig. S1 PXRD patterns of NU-1000.

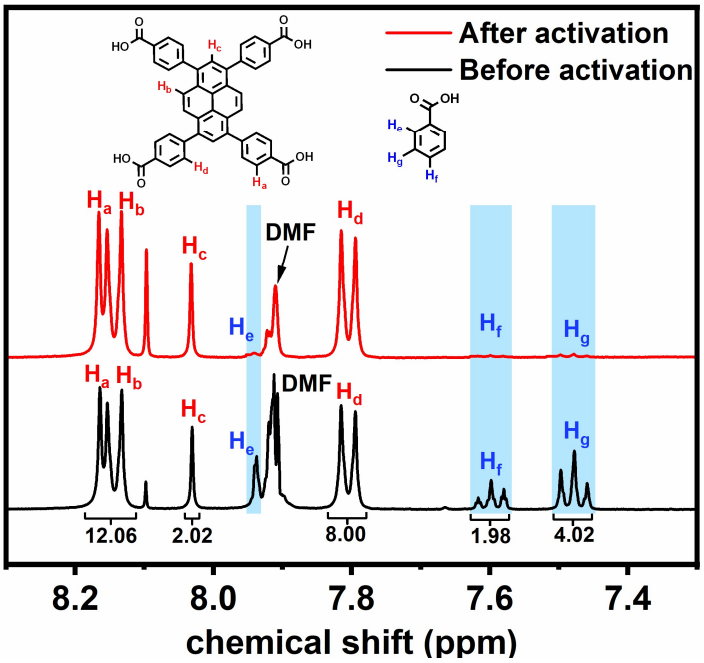

Fig. S2 Digestion ^{1}H NMR spectra of NU-1000 before activation and after HCl activation. The figure shows that the benzoic acid has been almost completely removed.

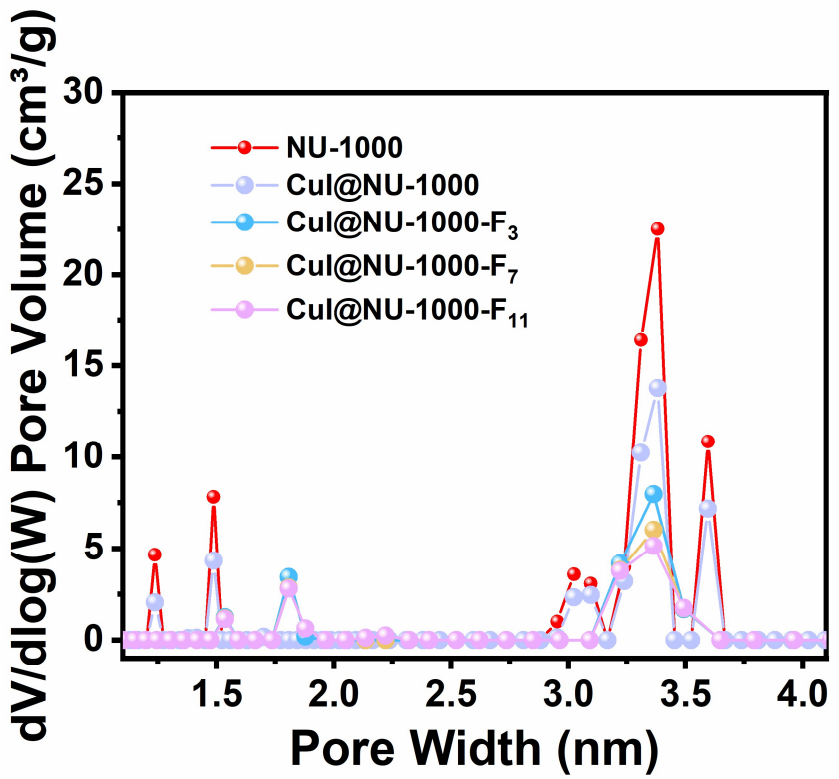

Fig. S3 Aperture distribution of NU-1000, CuI@NU-1000 and CuI@NU-1000-F_x (x= 3, 7, 11).

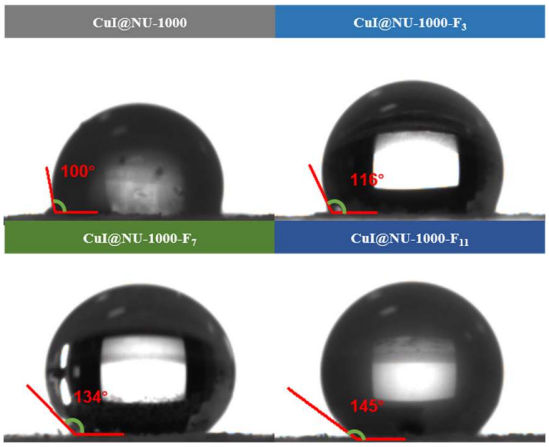

Fig. S4 Water contact angle of CuI@NU-1000 and CuI@NU-1000-F_x (x= 3, 7, 11).

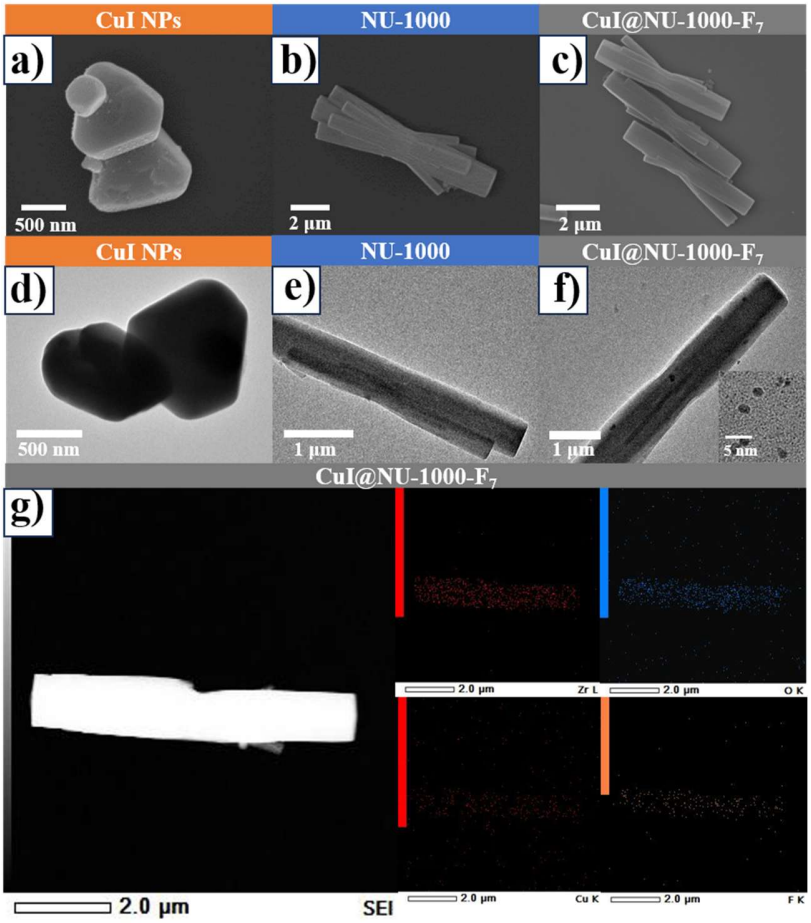

Fig. S5 Morphology and composition characterization of catalysts. (a-c) (a) SEM images of pristine CuI nanoparticles, (b) NU-1000, and (c) CuI@NU-1000-F_7. (d-f) (d) CuI NPs, (e) NU-1000, and (f) corresponding TEM images of CuI@NU-1000-F_7. (g) EDS elemental distribution map of CuI@NU-1000-F_7 showing the uniform distribution of Zr, O, Cu, and F elements.

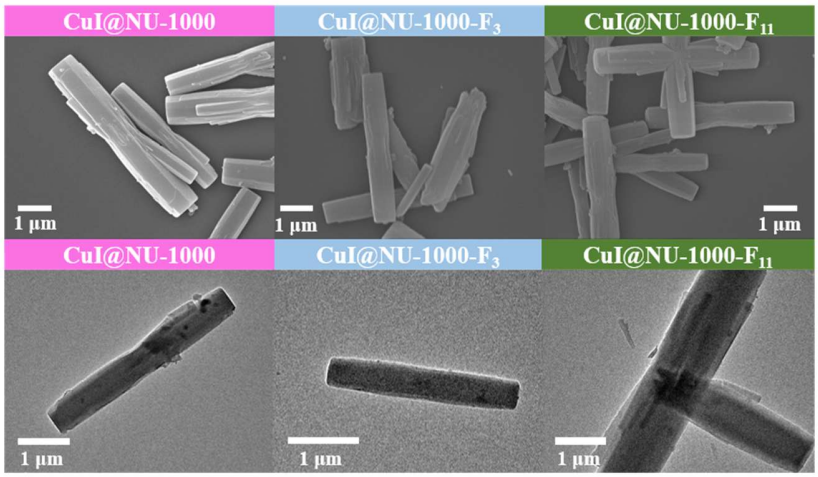

Fig. S6 (a) SEM images of CuI@NU-1000, (b) CuI@NU-1000-F_3, and (c) CuI@NU-1000-F_{11}. (d-f) (d) CuI@NU-1000, (e) CuI@NU-1000-F_3, and (f) corresponding TEM images of CuI@NU-1000-F_{11}.

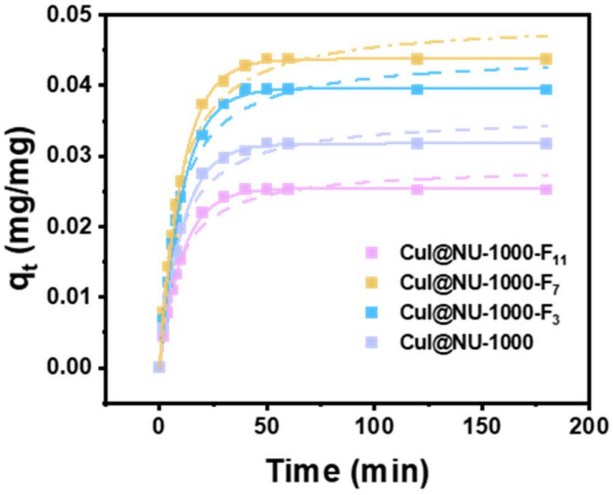

Fig. S7 Adsorption profiles of benzylamine.

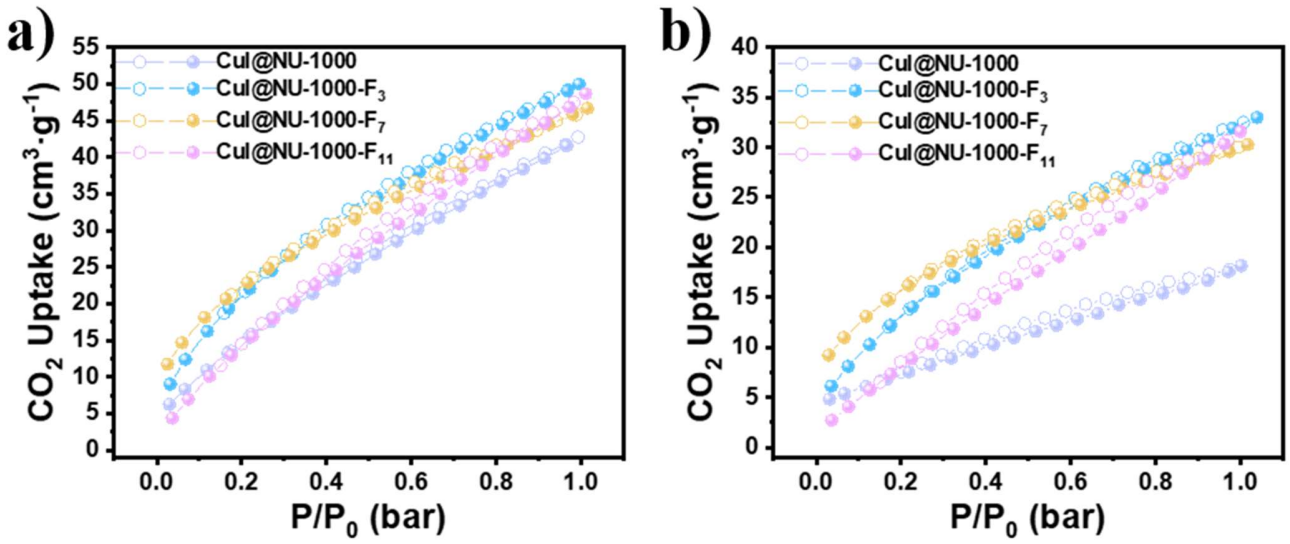

Fig. S8 CO_2 adsorption isotherms of the sample at 273 K (a) and 298 K (b)..

Section S3. Calculation of Isosteric Heat of Adsorption (Qst)

The isosteric heat of adsorption (Q_{st}) for CO_2 was calculated using the virial equation based on the adsorption isotherms measured at 273 and 298 K. The experimental data were fitted using the following virial equation:

$$\ln P = \ln N + 1/T \sum_{i=0}^{m} a_i N^i + \sum_{j=0}^{n} b_j N^j \text{ (Eq. S1)}$$

Where P is the pressure (measured in Pa), N is the amount adsorbed (measured in mmol/g), T is the temperature (measured in K), a_i and b_j are the virial coefficients, and m and n represent the number of coefficients required to adequately describe the isotherms.

Based on the fitting parameters obtained from Eq. S1, the isosteric heat of adsorption (Q_{st}) is dependent on the surface coverage and was calculated using the following equation:

$$Q_{st} = -R \sum_{i=0}^{m} a_i N^i \text{ (Eq. S2)}$$

Where R is the universal gas constant (8.314 $J \cdot mol^{-1} \cdot K^{-1}$).

The fitting results are shown in Fig . S6.

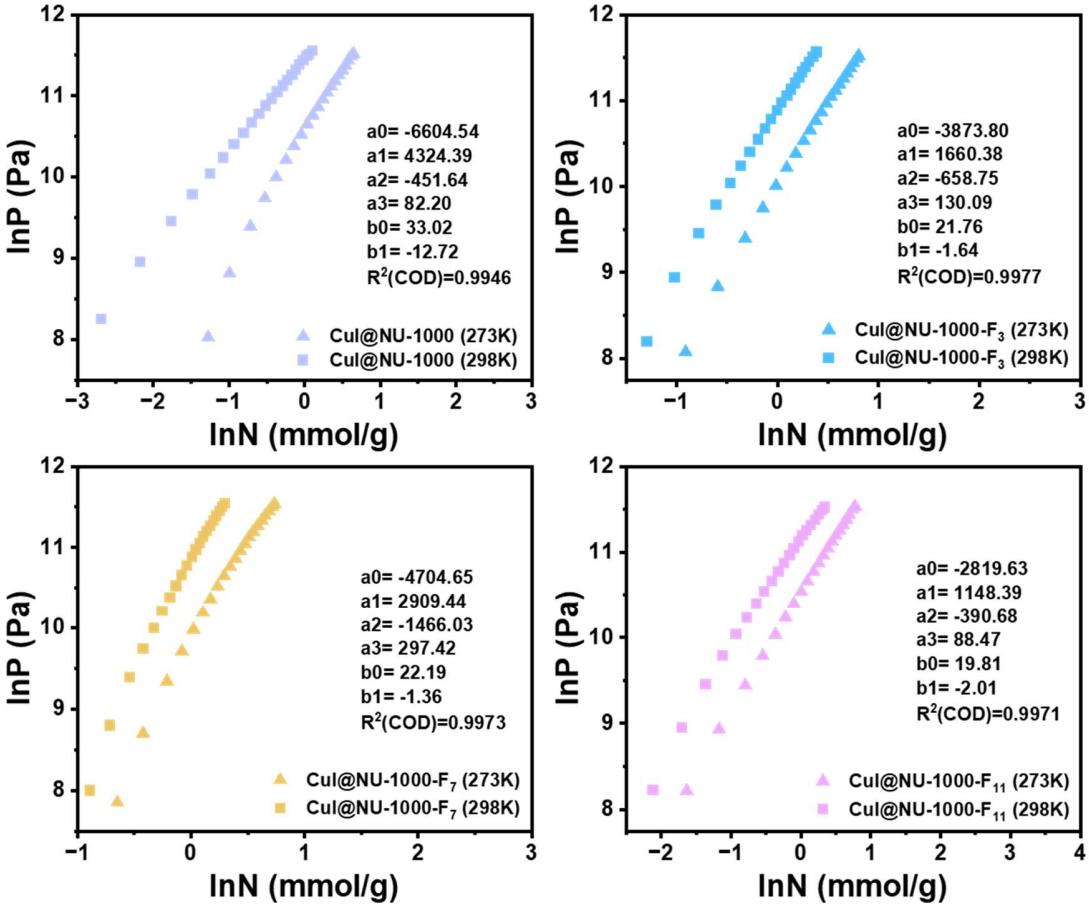

Fig. S9 Virial fitting of the CO_2 adsorption isotherms for CuI@NU-1000-F_x (x= 0, 3, 7, 11) at 273 and 298 K.

Section S4. Characterization of Catalytic Reaction Products

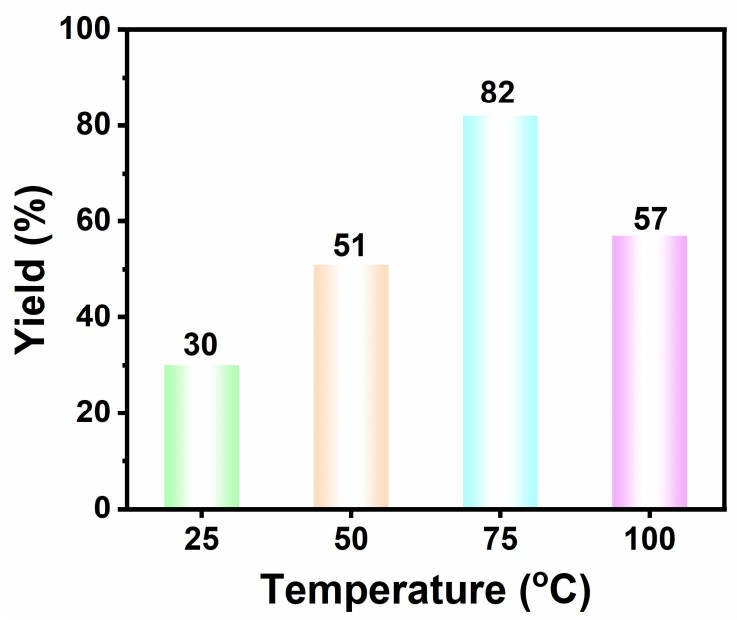

Fig. S10 Optimization of reaction temperature.

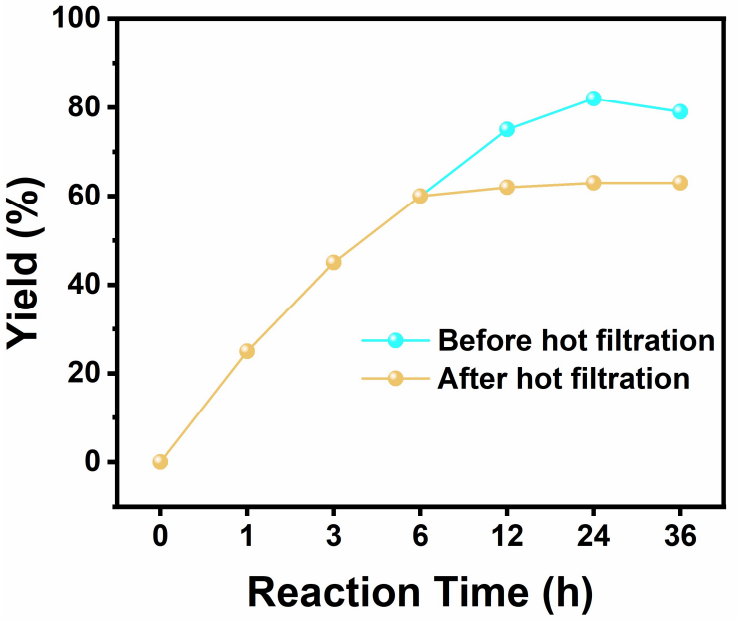

Fig. S11 The line graphs of heterogeneous test of CuI@NU-1000-F_7.

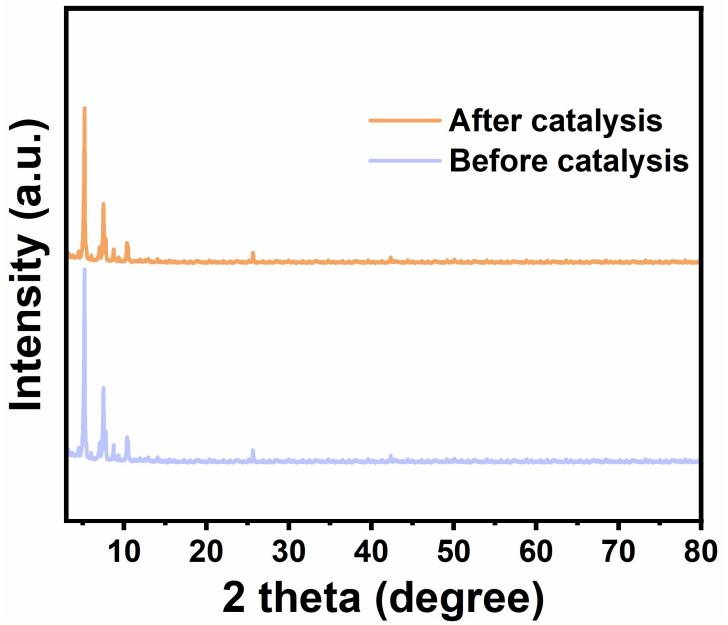

Fig. S12 XRD patterns of the catalyst before and after the catalytic reaction

Table 1: Substrate scope. [a]

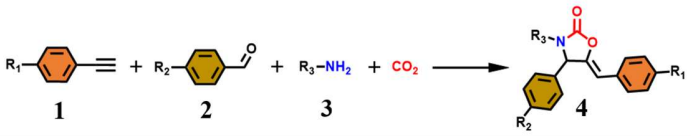

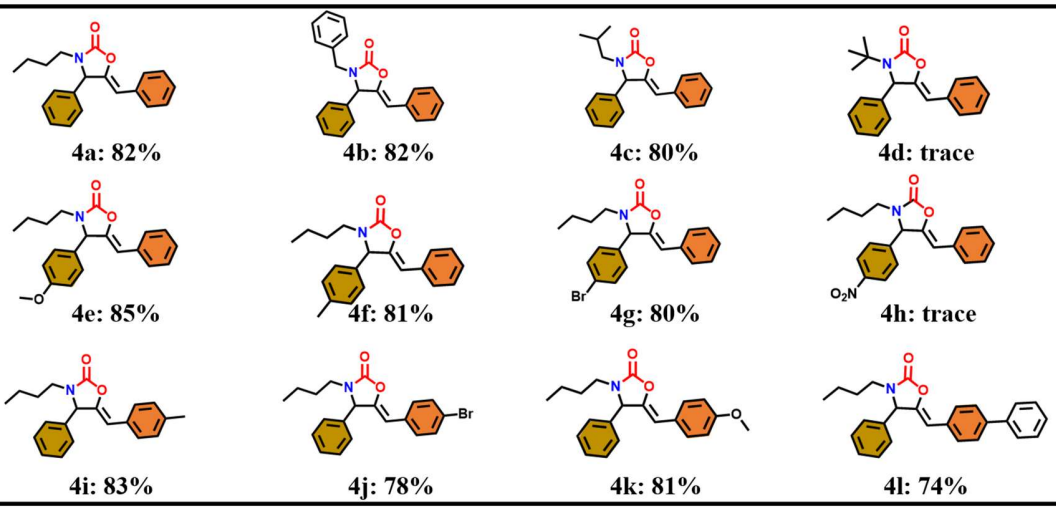

[a] Isolated yields.

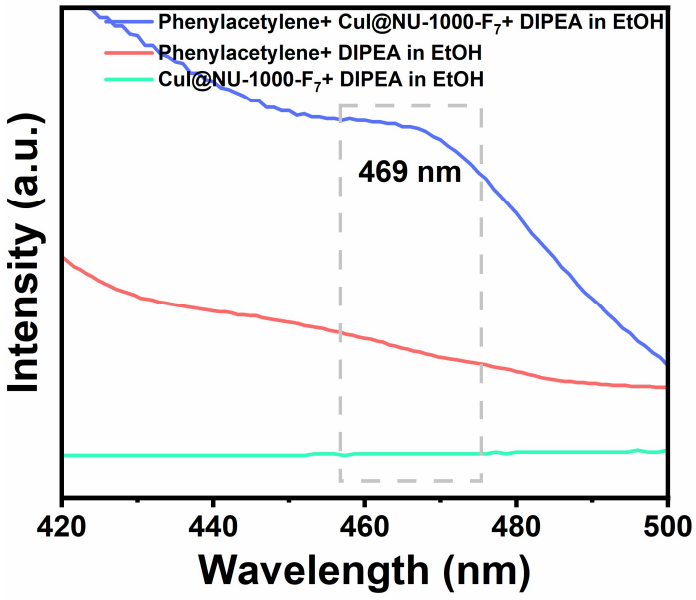

Fig. S13 UV–vis absorption spectra of in situ-generated Cu(I)-phenylacetylide in EtOH.

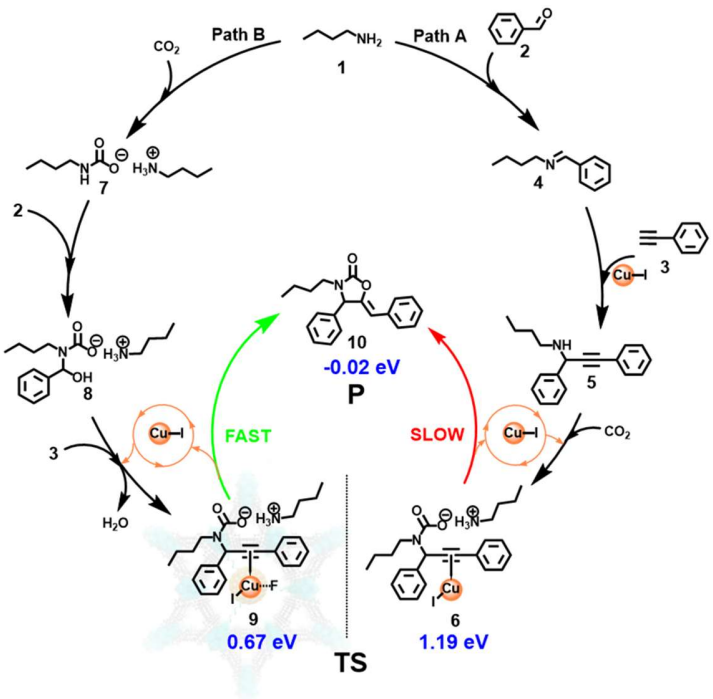

Fig. S14 Plausible mechanism for the formation of 10.

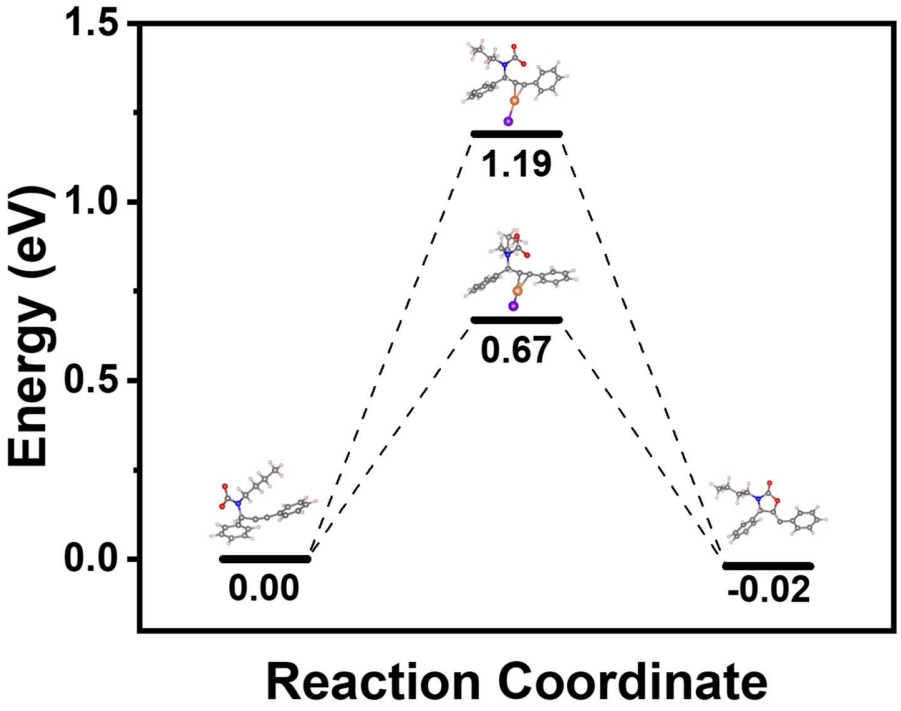

Fig. S15 Reaction energy profile for the cyclization of propargyl carbamate to oxazolidinone.Color codes: C, gray; H, white; O, red; N, blue; Cu, orange; I, purple; F, light green.

^{1}H NMR (400 MHz, $CDCl_3$) δ 7.51 (d, *J* = 7.5 Hz, 2H), 7.41 (d, *J* = 6.8 Hz, 3H), 7.34 – 7.23 (m, 4H), 7.16 (t, *J* = 7.4 Hz, 1H), 5.36 (d, *J* = 1.6 Hz, 1H), 5.24 (d, *J* = 1.8 Hz, 1H), 3.49 (dt, *J* = 15.4, 7.8 Hz, 1H), 2.81 (dt, *J* = 13.9, 7.5 Hz, 1H), 1.44 (p, *J* = 7.9 Hz, 2H), 1.27 (dt, *J* = 14.6, 6.6 Hz, 2H), 0.87 (t, *J* = 7.3 Hz, 3H).

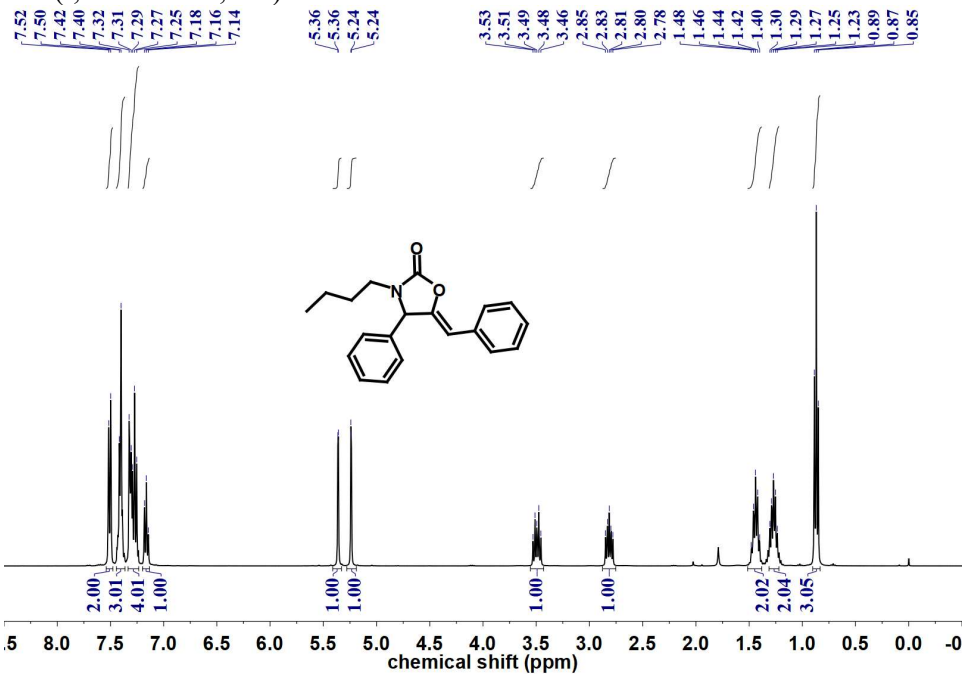

^{13}C NMR (101 MHz, $CDCl_3$) δ 155.06, 147.78, 137.36, 133.53, 129.39, 129.35, 128.46, 128.36, 127.83, 126.94, 104.54, 63.87, 41.65, 28.98, 19.82, 13.65.

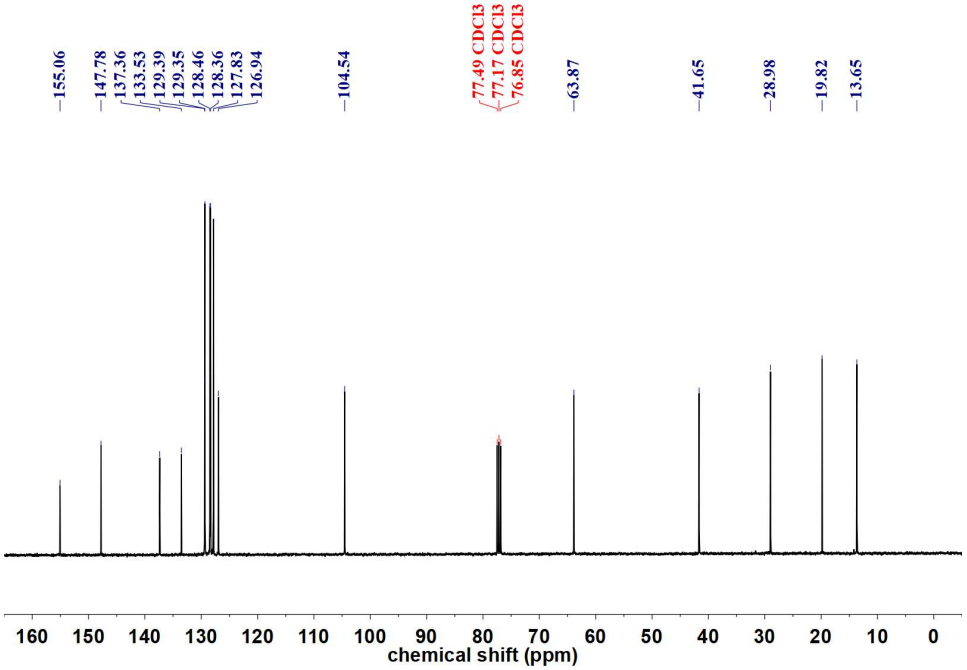

^{1}H NMR (400 MHz, $CDCl_3$) δ 7.55 (d, J = 7.5 Hz, 2H), 7.48 (dd, J = 5.0, 1.7 Hz, 3H), 7.41 – 7.28 (m, 7H), 7.23 (d, J = 7.6 Hz, 3H), 5.25 (d, J = 1.8 Hz, 1H), 5.19 (d, J = 1.6 Hz, 1H), 4.99 (d, J = 14.9 Hz, 1H), 3.74 (d, J = 15.0 Hz, 1H).

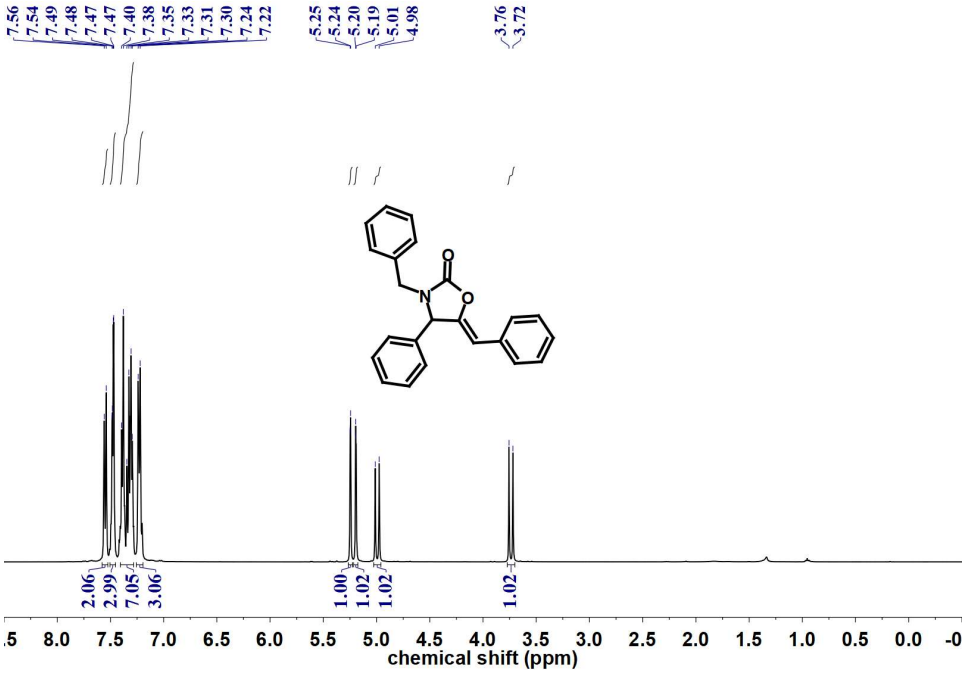

^{13}C NMR (101 MHz, $CDCl_3$) δ 155.15, 147.61, 136.84, 134.83, 133.42, 129.48, 129.41, 128.98, 128.65, 128.50, 128.40, 128.32, 128.11, 127.04, 104.88, 62.86, 45.60.

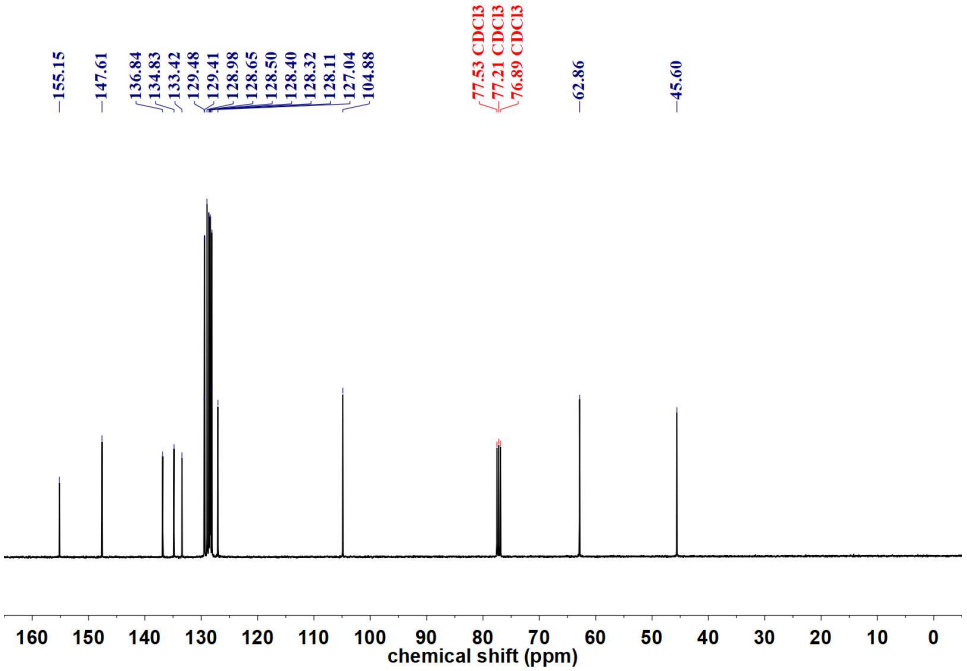

^{1}H NMR (400 MHz, $CDCl_3$) δ 7.55 (d, J = 7.5 Hz, 2H), 7.46 (d, J = 6.5 Hz, 3H), 7.37 – 7.29 (m, 4H), 7.21 (t, J = 7.4 Hz, 1H), 5.41 (d, J = 1.6 Hz, 1H), 5.29 (d, J = 1.8 Hz, 1H), 3.31 (dd, J = 14.1, 9.1 Hz, 1H), 2.68 (dd, J = 14.1, 6.0 Hz, 1H), 1.93 – 1.79 (m, 1H), 0.92 (dd, J = 14.2, 6.7 Hz, 6H).

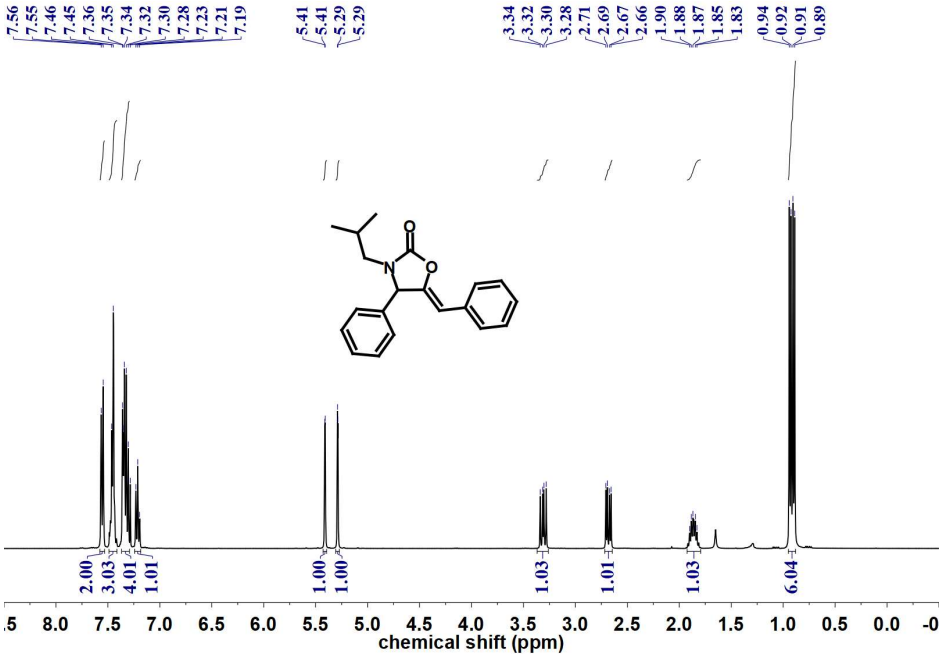

^{13}C NMR (101 MHz, $CDCl_3$) δ 155.37, 147.70, 137.27, 133.46, 129.40, 129.36, 128.46, 128.35, 127.83, 126.95, 104.54, 64.27, 49.18, 26.38, 20.17, 19.70.

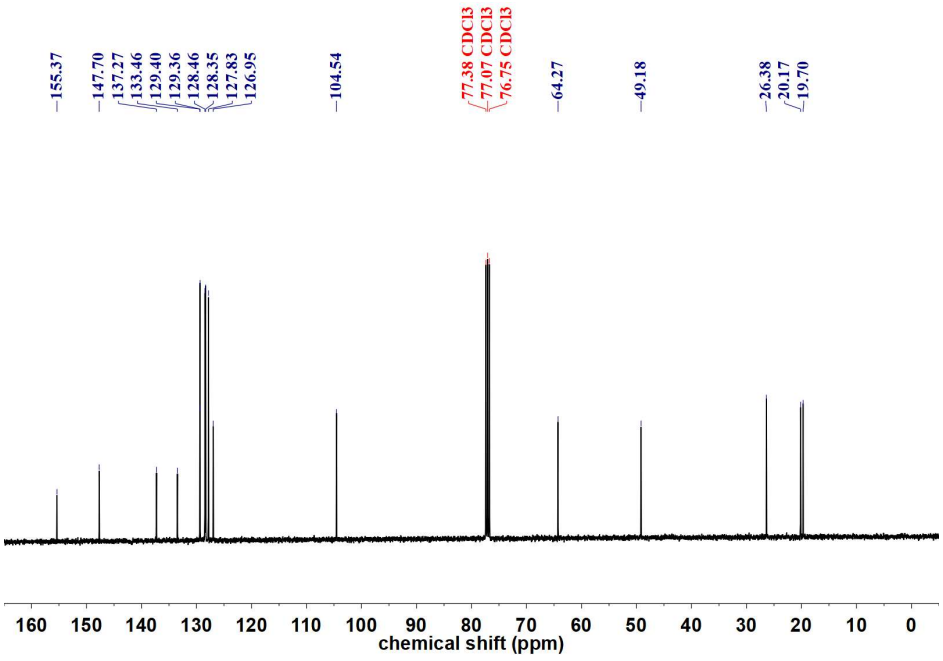

^{1}H NMR (400 MHz, $CDCl_3$) δ 7.44 (d, J = 7.8 Hz, 2H), 7.19 (dd, J = 12.7, 8.1 Hz, 4H), 7.10 (t, J = 7.3 Hz, 1H), 6.86 (d, J = 8.6 Hz, 2H), 5.27 (s, 1H), 5.16 (d, J = 1.5 Hz, 1H), 3.75 (s, 3H), 3.40 (dt, J = 14.7, 7.9 Hz, 1H), 2.74 (dt, J = 13.9, 7.5 Hz, 1H), 1.41 – 1.33 (m, 2H), 1.20 (dt, J = 14.5, 7.0 Hz, 2H), 0.80 (t, J = 7.3 Hz, 3H).

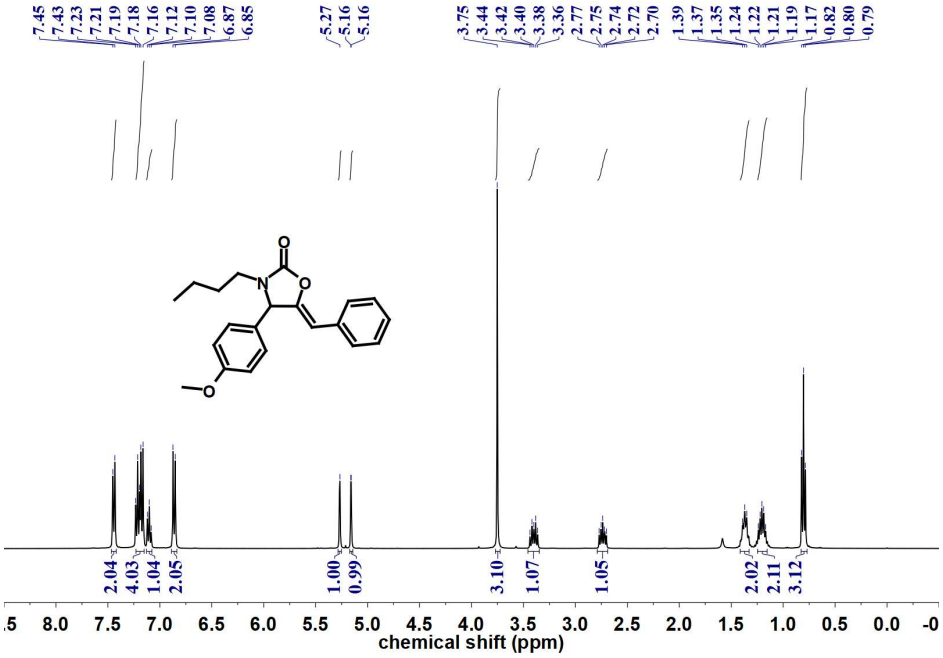

^{13}C NMR (101 MHz, $CDCl_3$) δ 160.34, 154.96, 148.15, 133.56, 129.22, 129.17, 128.45, 128.32, 126.87, 114.63, 104.34, 63.40, 55.39, 41.49, 28.97, 19.83, 13.67.

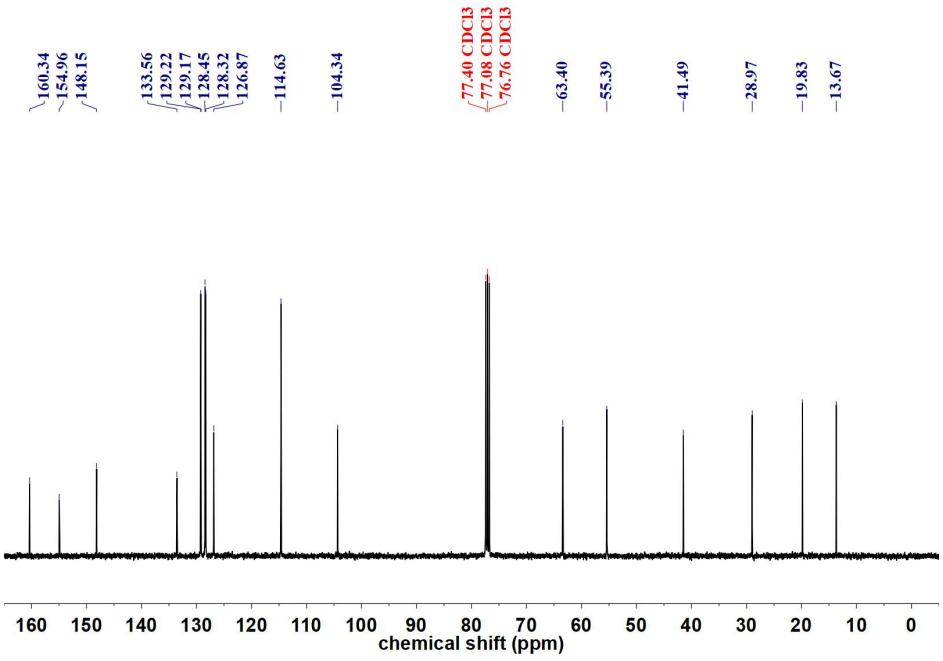

^{1}H NMR (400 MHz, $CDCl_3$) δ 7.55 (d, J = 7.6 Hz, 2H), 7.34 – 7.21 (m, 7H), 5.38 (d, J = 2.1 Hz, 1H), 5.27 (d, J = 2.0 Hz, 1H), 3.53 (dt, J = 15.3, 7.9 Hz, 1H), 2.83 (dt, J = 13.9, 6.7 Hz, 1H), 2.41 (s, 3H), 1.48 (p, J = 7.5, 6.7 Hz, 2H), 1.31 (dt, J = 14.6, 6.9 Hz, 2H), 0.91 (t, J = 7.3 Hz, 3H).

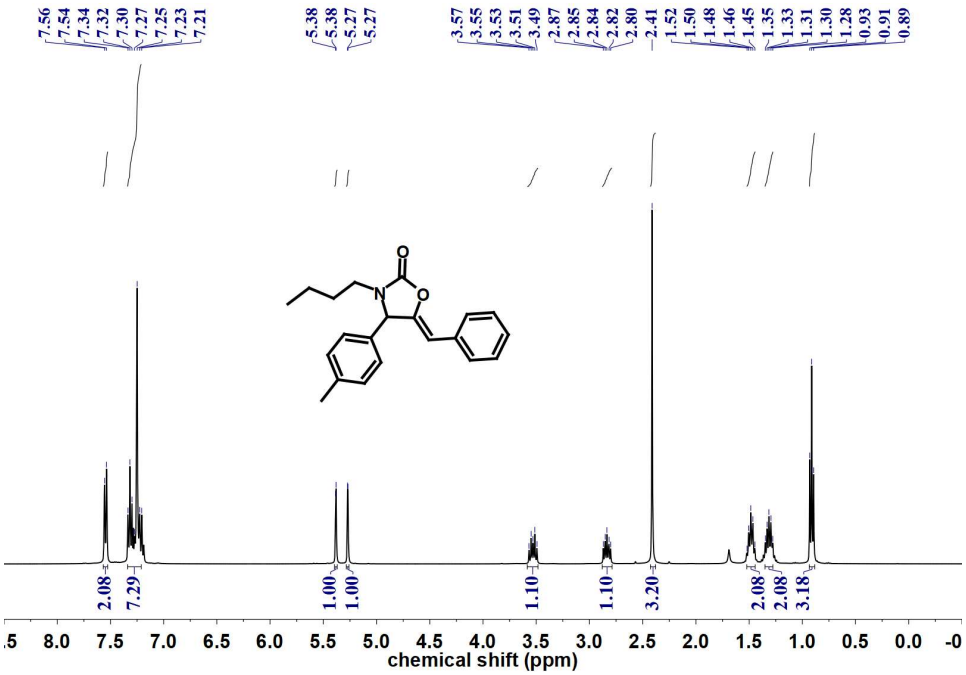

^{13}C NMR (101 MHz, $CDCl_3$) δ 155.06, 147.98, 139.36, 134.27, 133.55, 129.99, 128.44, 128.33, 127.78, 126.87, 104.35, 63.60, 41.51, 28.95, 21.28, 19.82, 13.67.

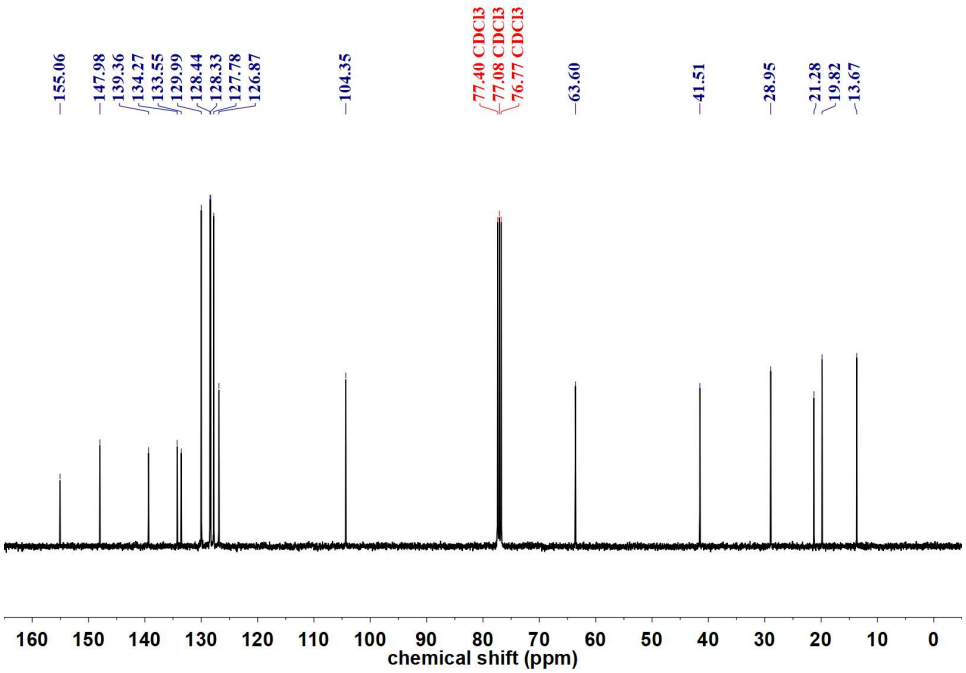

^{1}H NMR (400 MHz, $CDCl_3$) δ 7.50 (d, J = 8.4 Hz, 2H), 7.44 (d, J = 7.4 Hz, 2H), 7.22 (t, J = 7.6 Hz, 2H), 7.13 (dd, J = 14.0, 7.9 Hz, 3H), 5.28 (d, J = 1.8 Hz, 1H), 5.15 (d, J = 1.9 Hz, 1H), 3.49 – 3.39 (m, 1H), 2.79 – 2.69 (m, 1H), 1.43 – 1.33 (m, 2H), 1.24 – 1.18 (m, 2H), 0.82 (t, J = 7.3 Hz, 3H).

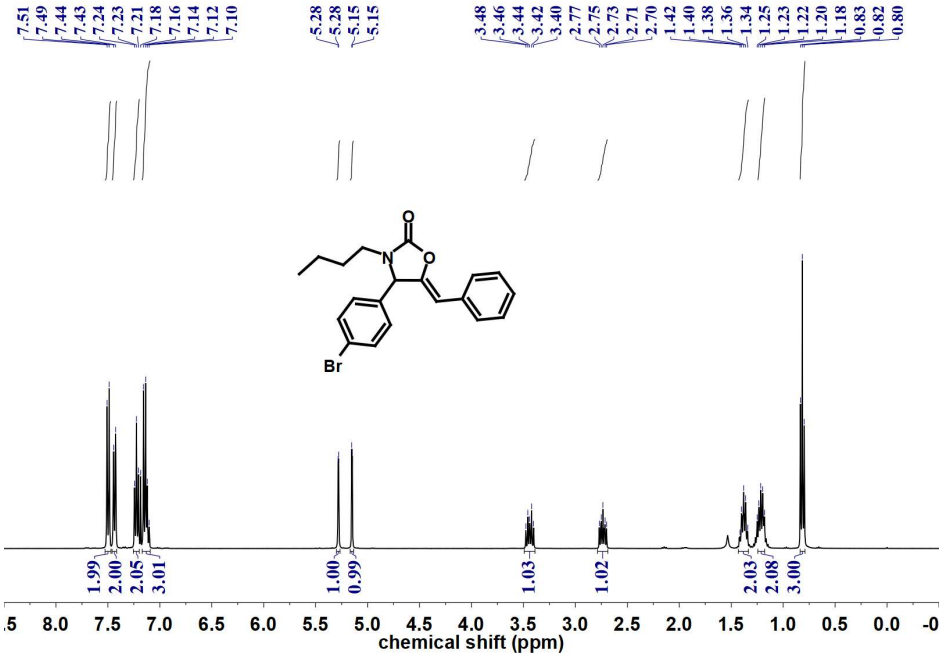

^{13}C NMR (101 MHz, $CDCl_3$) δ 154.89, 147.09, 136.41, 133.21, 132.59, 129.46, 128.50, 128.36, 127.13, 123.55, 104.89, 63.25, 41.69, 28.94, 19.80, 13.63.

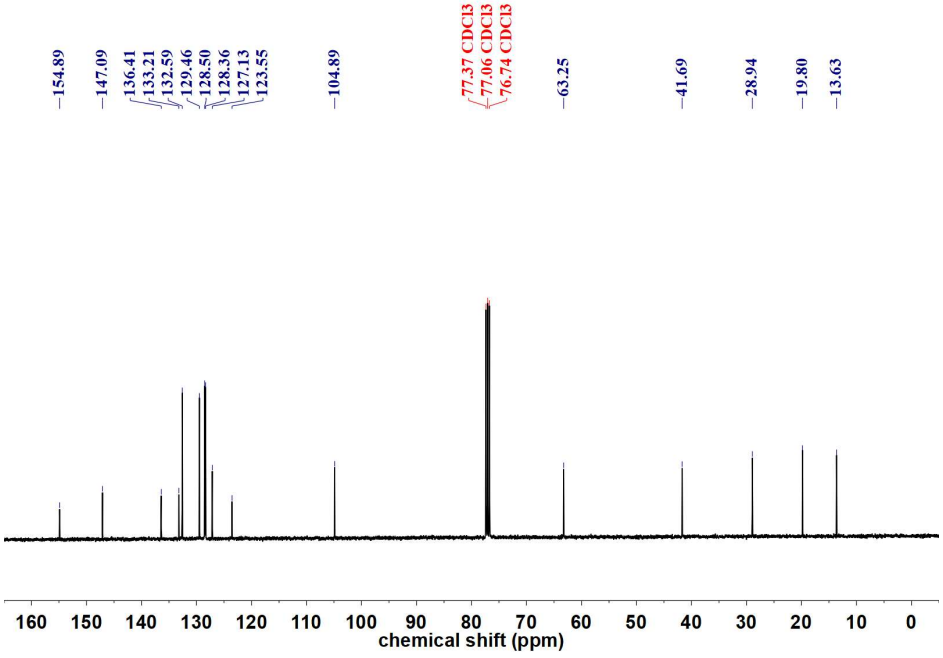

^{1}H NMR (400 MHz, $CDCl_3$) δ 7.48 – 7.42 (m, 5H), 7.35 (dd, J = 7.4, 2.0 Hz, 2H), 7.13 (d, J = 8.0 Hz, 2H), 5.40 (d, J = 1.6 Hz, 1H), 5.25 (d, J = 1.9 Hz, 1H), 3.59 – 3.48 (m, 1H), 2.90 – 2.80 (m, 1H), 2.34 (s, 3H), 1.53 – 1.43 (m, 2H), 1.31 (dt, J = 14.7, 6.6 Hz, 2H), 0.91 (t, J = 7.3 Hz, 3H).

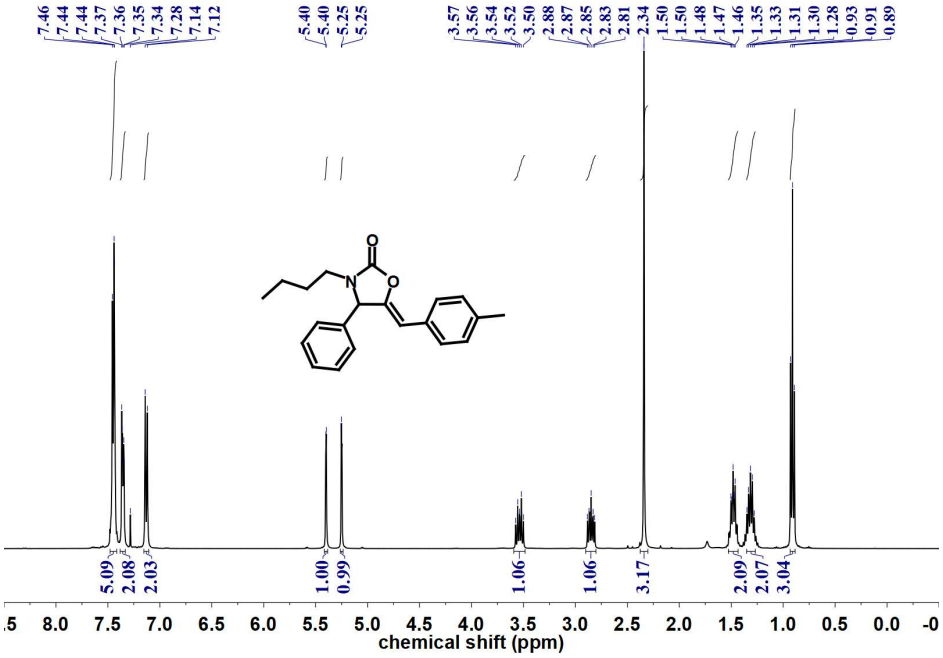

^{13}C NMR (101 MHz, $CDCl_3$) δ 155.18, 146.98, 137.47, 136.76, 130.65, 129.33, 129.30, 129.16, 128.27, 127.84, 104.50, 63.83, 41.62, 28.97, 21.24, 19.82, 13.65.

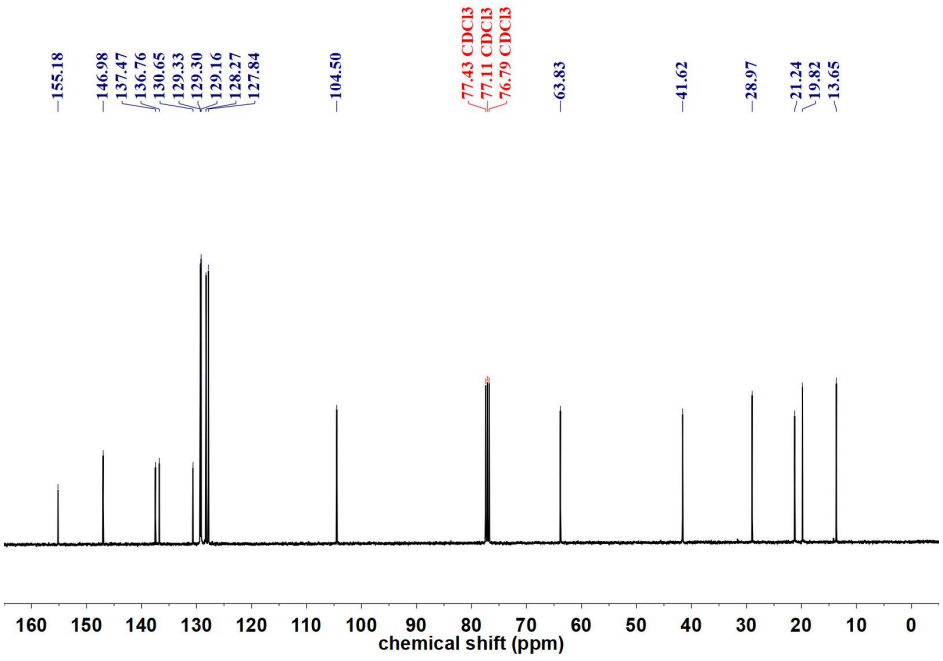

^{1}H NMR (400 MHz, $CDCl_3$) δ 7.44 (s, 2H), 7.40 (s, 4H), 7.34 (dd, J = 7.3, 2.0 Hz, 2H), 5.38 (d, J = 1.8 Hz, 1H), 5.21 (d, J = 1.9 Hz, 1H), 3.53 (dt, J = 15.4, 7.8 Hz, 1H), 2.89 – 2.80 (m, 1H), 1.52 – 1.42 (m, 2H), 1.30 (dt, J = 14.7, 6.6 Hz, 2H), 0.90 (t, J = 7.3 Hz, 3H).

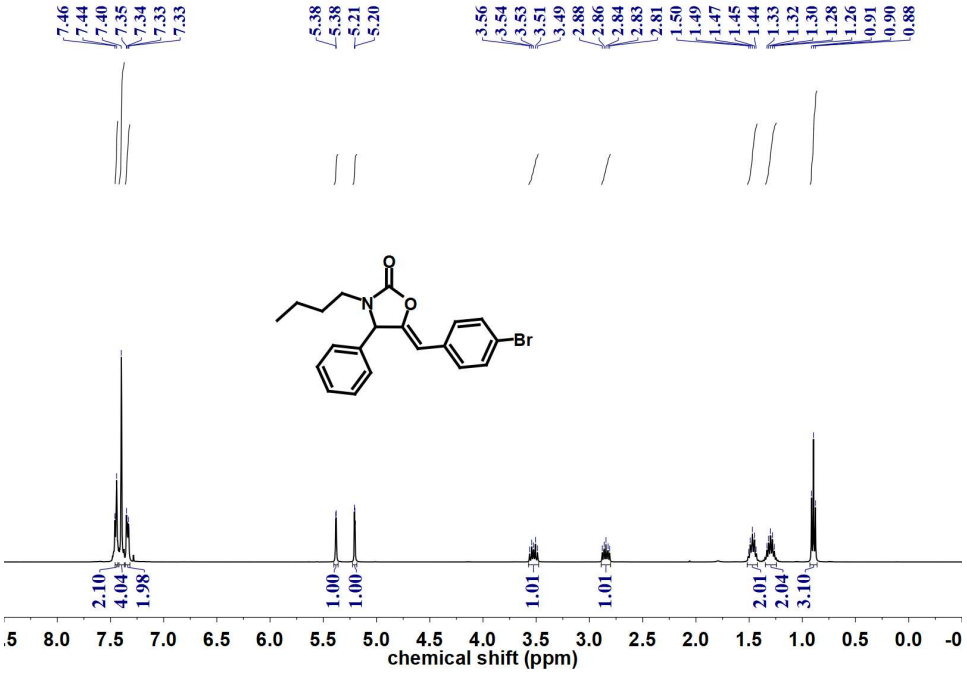

^{13}C NMR (101 MHz, $CDCl_3$) δ 154.78, 148.46, 137.02, 132.48, 131.51, 129.87, 129.50, 129.42, 127.78, 120.61, 103.39, 63.89, 41.67, 28.94, 19.81, 13.65.

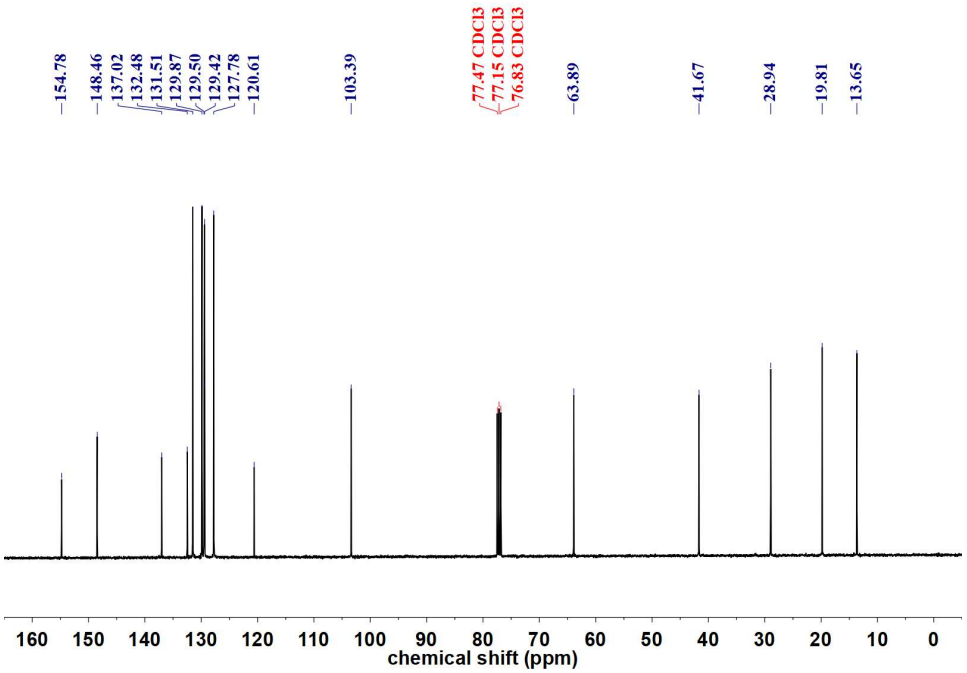

^{1}H NMR (400 MHz, $CDCl_3$) δ 7.45 (dd, J = 19.5, 7.8 Hz, 5H), 7.34 (d, J = 7.7 Hz, 2H), 6.84 (d, J = 8.8 Hz, 2H), 5.39 – 5.36 (m, 1H), 5.22 (d, J = 1.5 Hz, 1H), 3.78 (s, 3H), 3.51 (dt, J = 15.1, 7.8 Hz, 1H), 2.84 (dt, J = 13.9, 6.7 Hz, 1H), 1.50 – 1.42 (m, 2H), 1.29 (dt, J = 14.6, 6.8 Hz, 2H), 0.89 (t, J = 7.3 Hz, 3H).

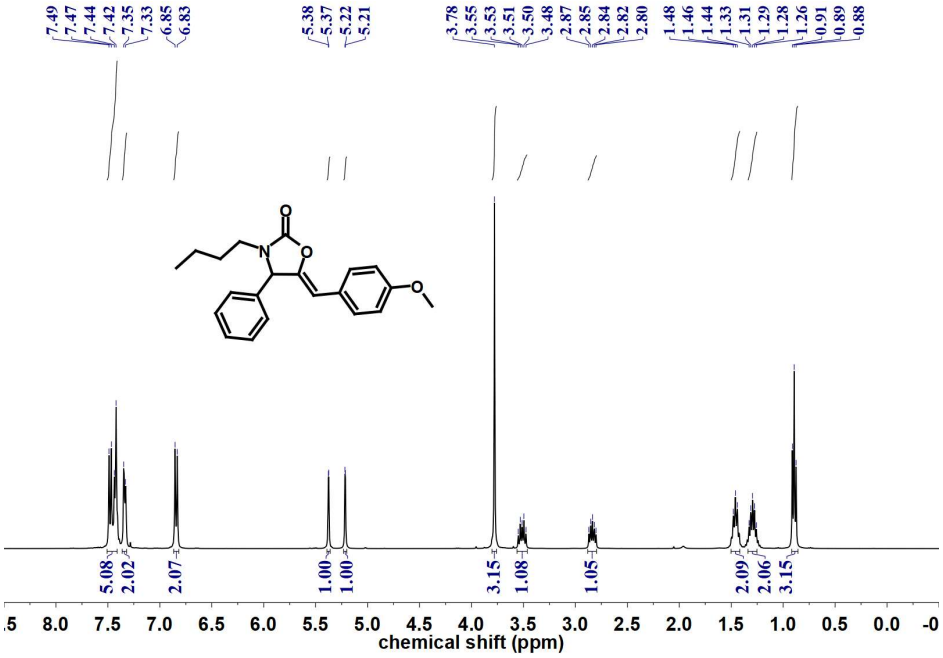

^{13}C NMR (101 MHz, $CDCl_3$) δ 158.48, 155.22, 146.06, 137.56, 129.64, 129.30, 127.82, 126.29, 113.86, 104.08, 63.76, 55.23, 41.61, 28.95, 19.81, 13.66.

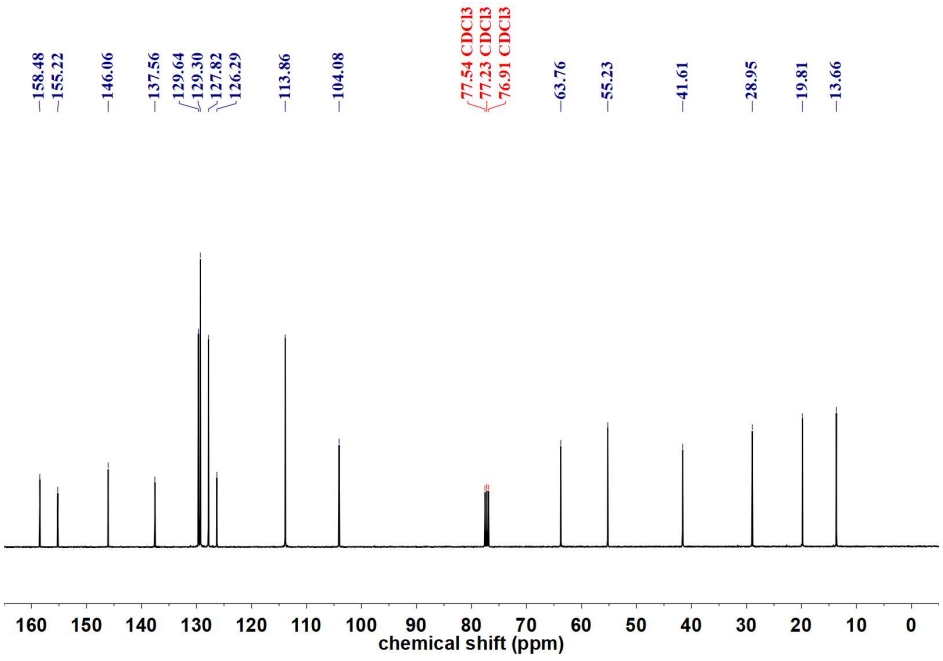

^{1}H NMR (400 MHz, $CDCl_3$) δ 7.64 (t, J = 7.2 Hz, 4H), 7.58 (d, J = 8.4 Hz, 2H), 7.49 – 7.44 (m, 5H), 7.38 (dd, J = 7.6, 2.1 Hz, 3H), 5.44 (d, J = 1.8 Hz, 1H), 5.33 (d, J = 1.9 Hz, 1H), 3.61 – 3.52 (m, 1H), 2.92 – 2.83 (m, 1H), 1.55 – 1.46 (m, 2H), 1.33 (dt, J = 14.7, 7.2 Hz, 2H), 0.93 (t, J = 7.3 Hz, 3H).

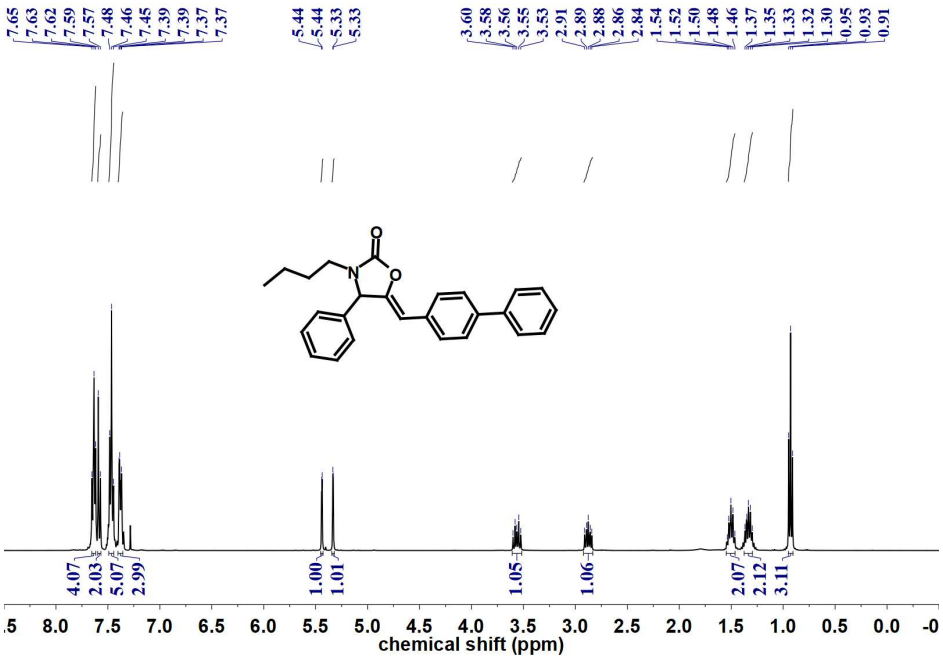

^{13}C NMR (101 MHz, $CDCl_3$) δ 155.06, 147.95, 140.67, 139.55, 137.33, 132.61, 129.43, 129.38, 128.82, 128.79, 127.86, 127.33, 127.10, 126.96, 104.19, 63.93, 41.67, 28.99, 19.84, 13.68.

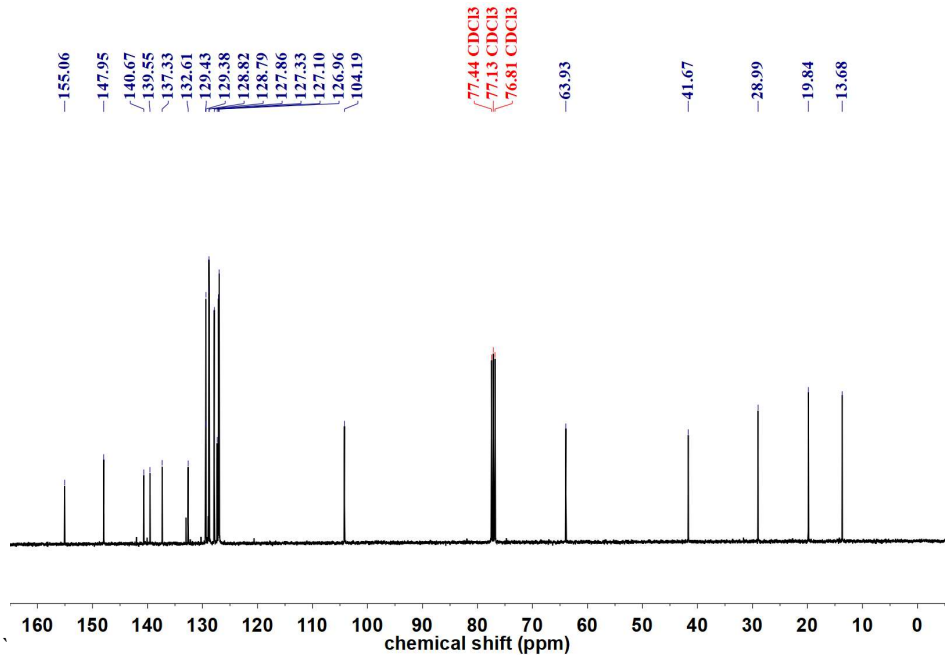

References

S1 S. Gao, Z. Li, X. Jia, K. Jiang and H. Zeng, *Green Chem.*, 2010, **12**, 1442–1447.

S2 P. Deria, J. E. Mondloch, E. Tylianakis, P. Ghosh, W. Bury, R. Q. Snurr, J. T. Hupp and O. K. Farha, *J. Am. Chem. Soc.*, 2013, **135**, 16801–16804.

S3 W.-J. Yoo and C.-J. Li, *Adv. Synth. Catal.*, 2008, **350**, 1503–1506.